

MULTI-FREQUENCY MEMS-BASED ELECTROMAGNETIC ENERGY HARVESTER

Huicong Liu¹, Lokesh Dhakar^{1,2}, and Chengkuo Lee¹

¹Department of Electrical and Computer Engineering, National University of Singapore, Singapore

²NUS Graduate School for Integrative Sciences and Engineering, National University of Singapore, Singapore

Abstract: A novel MEMS energy harvester (EH) has been proposed and fabricated in order to harvest energy from three dimensional (3-D) vibrations and multiple frequencies. It comprises of circular ring shaped springs, circular proof mass coated with two-layered aluminum coils, and a permanent magnet. The device exhibits the first resonant mode of 1285 Hz in the out-of-plane direction. The second and third modes are along the plane of device at frequencies of 1470 and 1550 Hz, respectively. The optimum power of these three modes is measured to be 0.016, 0.0087 and 0.0045 μW , respectively.

Keywords: Electromagnetic, energy harvester, MEMS, 3-D vibrations.

INTRODUCTION

Energy harvesting from the environmental vibrations has emerged as a research area in past few years and is considered as a promising solution to power wireless sensors and biomedical devices without using a battery. MEMS based energy harvesters (EHs) typically use piezoelectric, electromagnetic and electrostatic mechanisms to convert kinetic energy to electrical energy. Most of the resonant based EHs produce usable power only in the first mode with a narrow bandwidth. In the cantilever type EHs, the highest power output occurs at the first out-of-plane mechanical resonance [1-2], while the in-plane energy harvesting structures deploy springs of low stiffness in order to enlarge the in-plane displacement [3-4]. In both cases, significant energy can only be scavenged in one resonant frequency and usually along one specific direction. But in reality, the vibration sources may exhibit several frequency peaks in different directions. Therefore it is desirable to design EHs which can harvest vibration in 3-D and at various resonant frequencies.

To solve the problem of harvesting energy at different frequencies, there have been many prototypes built using the frequency tunable and wideband approaches [5-6]. Wideband EHs have been reported by using magnets [7], mechanical stoppers [8] and nonlinear springs [9], to collect energy within a continuous frequency range rather than from discrete frequency peaks spreading over a wide range. However, many vibration sources exhibit different vibration peaks at various frequencies, e.g. a HVAC vent exhibits three discrete frequency peaks of 21.8, 29 and 127.3 Hz according to Reilly's survey [10]. A Statasys 3D printer exhibits three frequency peaks of

28 (1-axis), 28.3 (2-axis) and 44.1 Hz (3-axis) along different axes. A W500 Lenovo laptop exhibits two frequency peaks of 85.2 and 119 Hz along two axes. In this paper, we present a fabricated MEMS device as a potential solution to the problem of harvesting energy from 3-D vibrations at discrete frequencies. The device can harvest energy from out-of-plane vibration at mode I (1285 Hz), in-plane vibrations at modes II (1470 Hz) and III (1550 Hz). The power densities achieved for the three modes are 0.444, 0.242 and 0.125 $\mu\text{W}/\text{cm}^3$, respectively, at an excitation acceleration of 1g.

DEVICE DESIGN AND FABRICATION

The schematic diagram of a 3-D electromagnetic EH chip is shown in Fig. 1(a). The MEMS EH chip consists of a movable circular mass with a diameter of 4.5 mm and a thickness of 450 μm suspended by circular ring shaped springs. There are three concentric circular rings, each with a width of 30 μm and a height of 150 μm . The rings are connected to each other at a spacing of 200 μm by junction blocks which are placed at an interval of 60° in the alternate gaps between the three rings. There are three diamond shaped Al coils namely coil 1, 2 and 3 deposited on the circular proof mass symmetrically at an angle of 120°. All three coils consist of two layers and each layer comprises 17 loops of 1x10 μm wires separated by a gap of 25 μm . Each coil is connected to separate set of bonding pads as shown in Fig. 1(a). The MEMS EH chip is then assembled onto a dual in-line package (DIP) base separated by a spacer. As shown in Fig. 1(b), a permanent NdFeB magnet with a diameter of 3 mm and height of 2 mm is attached on a supporting beam structure. The magnet is on top of the EH chip

with a gap of 1mm. The coils generate induced emf according to Faraday’s law of induction when the proof mass moves in the magnetic field.

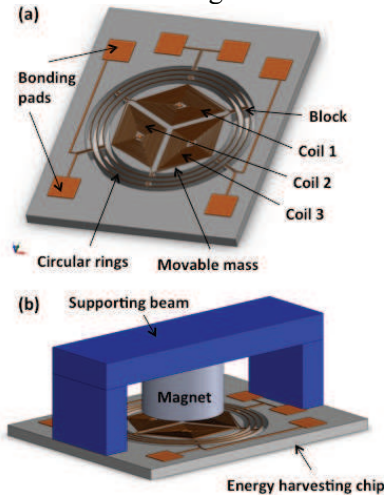


Fig. 1: (a) Schematic diagram of the proposed EH (b) EH assembled with a permanent magnet.

As shown in Fig. 2, the fabrication process starts from a SOI wafer which has a 150 μm thick Si device layer, a 1 μm thick buried oxide (BOX) layer and a 725 μm thick Si handling layer. The SOI wafer is first covered with a 0.1 μm thick Si_3N_4 insulation layer using a plasma-enhanced chemical vapor deposition (PECVD) system [Fig. 2(a)]. Then a 1 μm thick Al layer is deposited by physical vapor deposition (PVD) followed by reactive ion etching (RIE) to pattern first coil layer and bonding pads (Mask 1) [Fig. 2(b)]. Then, a 0.8 μm thick Si_3N_4 insulation layer is deposited by PECVD and pad openings are patterned (Mask 2) [Fig. 2(c)]. Thereafter, 1 μm thick Al and 0.8 μm thick Si_3N_4 layers are deposited and patterned (Mask 3 and 4 respectively) followed by etching to form second coil layer and contact pads [Fig. 2(d)]. Then a 2 μm thick SiO_2 layer is deposited on the top surface as a passivation and hard mask layer, followed by patterning (Mask 5) and RIE of the SiO_2 , Si_3N_4 layers using CHF_3 (for SiO_2) and CF_4 (for Si_3N_4). A Si device layer with depth of 150 μm is then done by deep RIE, i.e., DRIE, to form the circular-mass and concentric circular rings [Fig. 2(e)].

After completing the front-side processes, the Si handling layer is reduced to 300 μm using backside grinding and polishing. Then a 2 μm SiO_2 layer is deposited and patterned (Mask 6) on the backside of the wafer [Fig. 2(f)]. The backside DRIE is used to etch a trench up to depth of 250 μm [Fig. 2(g)]. Several fine DRIE steps are performed to remove the remaining 50 μm of Si handling layer. Finally, the remaining SiO_2 on the front-side and BOX layers are etched away by CHF_3 plasma [Fig. 2(h)].

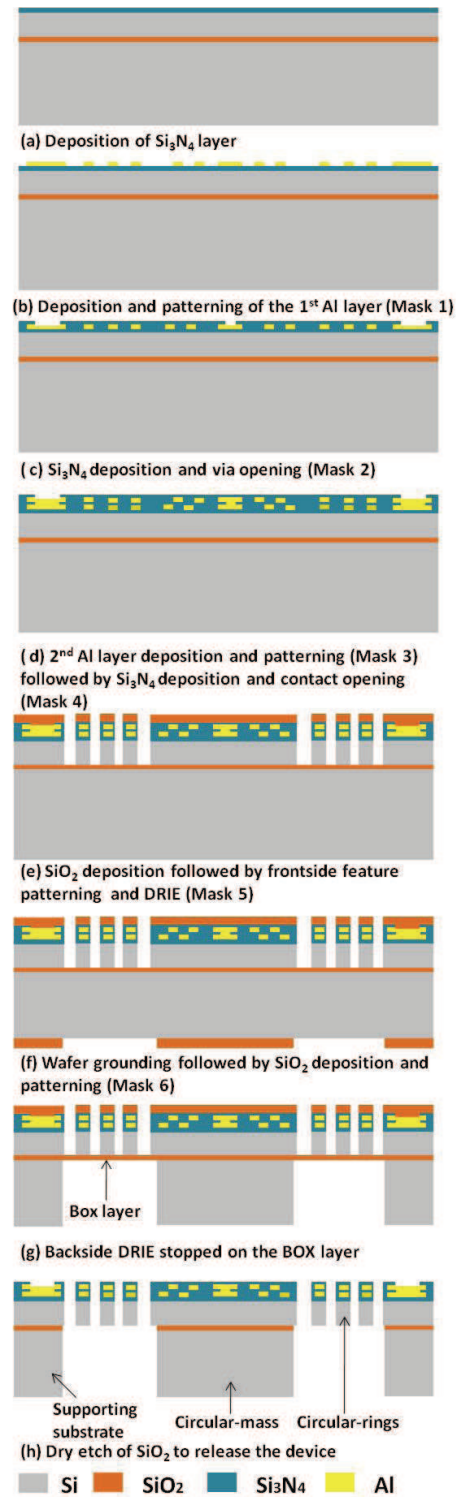


Fig. 2: Fabrication process of the electromagnetic EH chip

Fig. 3(a) shows the final released EH device assembled on a DIP connected with bonding pads using gold wires. A SEM image of the circular rings and circular mass is shown in Fig. 3(b). In the final fabricated device, the width of circular-ring is 20-25 μm instead of 30 μm . Due to the variations in the

actual fabricated device, the height of the circular mass is found to be reduced to 400 μm due to over etching in backside DRIE process. The circular rings also display unsymmetrical undercuts resulting into changes in resonant axes and frequencies [11].

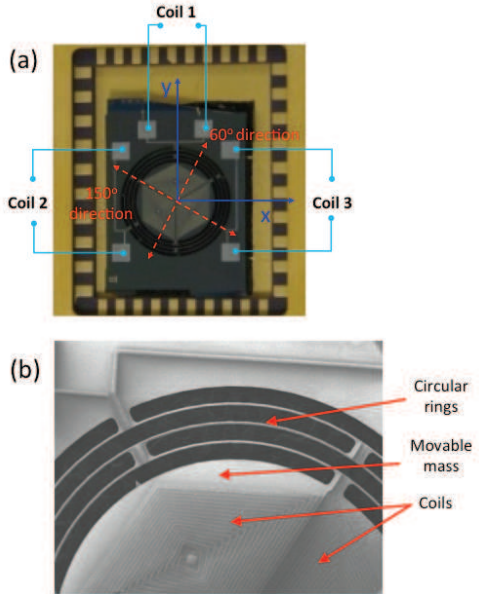


Fig. 3 (a) EH assembled on a DIP (b) SEM image of the EH.

EXPERIMENTAL RESULTS

To characterize the EH, it was mounted on a shaker and excited with various frequencies, amplitudes in different directions. The output voltages generated by three different coils were then recorded using different channels of dynamic signal analyzer. The out-of-plane mode and in-plane modes were characterized.

Out-of-plane motion (mode I)

The EH was excited at frequencies from 1200 to 1400 Hz at 1 g acceleration along the out-of-plane direction. In the out-of-plane mode I, all three coils move symmetrically with respect to the magnet resulting in similar magnetic flux changes. Fig. 4(a) show the similar output voltages of coils 1, 2 and 3 (3.5~3.6 mV) at resonant frequency of 1285 Hz. These three coils at mode I at an acceleration of 1 g gives an overall output power against load resistance as shown in Fig. 4(b). The maximum power output of 0.016 μW is generated when the load resistance matches with the impedance of EH at 1.8 k Ω , from which an equivalent power density of 0.444 $\mu\text{W}/\text{cm}^3$ could be obtained.

In-plane motion (modes II and III)

To characterize the in-plane modes, output voltages from the coils were measured for frequencies 1200-1700 Hz at 1 g acceleration along in-plane directions

with an increment of 30° in the range of 0° to 180°. The resonance modes II (1470 Hz) and III (1550 Hz) occur at an angle of 60° and 150° respectively [Fig. 5(a) and (b)]. For mode II, coils 1 and 2 show similar output characteristics with maximum output voltages of 3.6 and 2.9 mV respectively, and coil 3 generates negligible output voltage compared to the other two coils. The output voltages of coils 1 and 2 decrease continuously as the excitation angle varies from 60° to 150°. When mode III resonance is excited at an angle of 150°, coils 1, 2 and 3 produce maximum output voltage of 1.1, 1.3 and 2.6 mV [Fig. 5(b)]. The minimum output voltage from the three coils is approximately 0.2-0.3 mV at a perpendicular excitation angle of 60°.

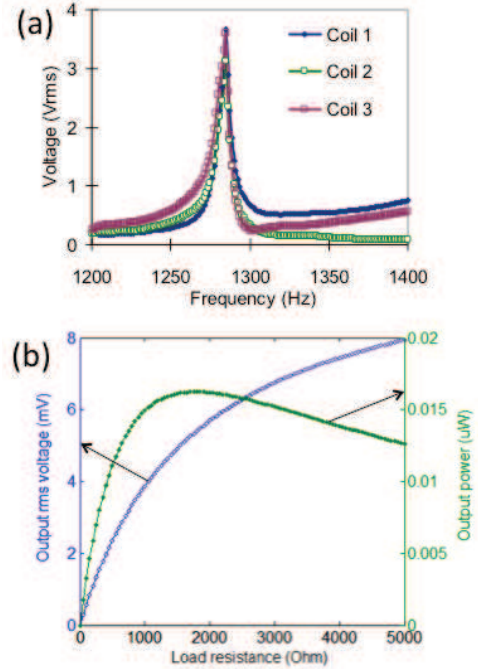


Fig.4: (a) Output voltages (in mV) of coils 1,2 and 3 for mode I (b) Overall output voltage and power of EH.

It is observed that the coils 1 and 2 show similar behavior for modes II and III. This can be explained by the similar positioning of coils 1 and 2 with respect to both 60° and 150° directions, the angles at which in-plane resonance occurs. As long as the variation of the magnetic field due to a cylindrical magnet is in the radial direction and not in the angular direction, the flux change in coils 1 and 2 are similar. The negligible output of coil 3 for mode II (60°) can be explained by the symmetry of the coil with respect to 60° direction [Fig. 3] which results in minimum change of flux in coil. The maximum change in flux occurs at mode III as the circular mass moves in the 150° direction. In mode III, the output voltage of coil 3 is twice the output voltage of coil 1 and 2. The optimum power of

each coil occurs when the load resistance matches with the resistance of coil. The overall optimum power (combined for coils 1, 2 and 3) and power density for modes II and III are shown in Fig. 6(a) and (b), respectively. For mode II, the maximum power and power density are measured to be $0.0087 \mu\text{W}$ and $0.242 \mu\text{W}/\text{cm}^3$, respectively. Similarly for mode III, the maximum power and power density are $0.0045 \mu\text{W}$ and $0.125 \mu\text{W}/\text{cm}^3$, respectively.

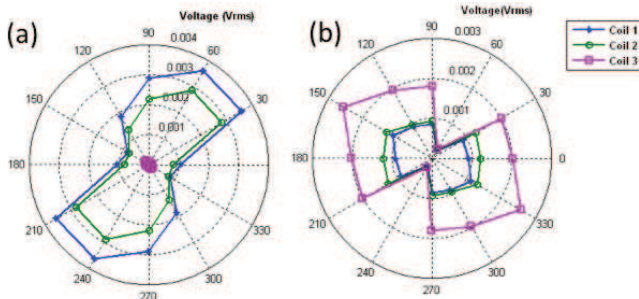


Fig. 5: Voltages (in V) for (a) mode II and (b) mode III.

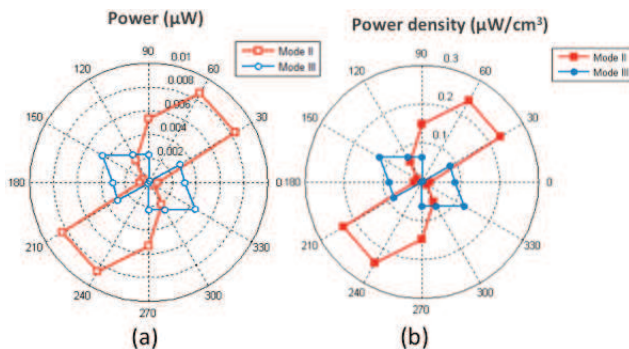


Fig. 6: (a) Overall power and (b) power density for modes II and III.

CONCLUSION

A novel electromagnetic MEMS EH is designed and fabricated in order to scavenge energy from 3-D vibrations. The first three resonance modes of EH are characterized at frequencies of 1285, 1470 and 1500 Hz under vibrations of 1 g acceleration in various directions, while the overall optimal power for three modes is measured to be 0.016, 0.0087 and $0.0045 \mu\text{W}$, respectively. The power output of the presented EH can be further improved by increasing the number of coils and magnetic field strength. The present preliminary data prove that scavenging energy from 3-D vibrations is a feasible EH mechanism.

ACKNOWLEDGEMENT

This work is partially supported by Faculty Research Committee (FRC) Grant (No. R-263-000-692-112) at the National University of Singapore, and Project 2 -

Energy harvesting solutions for wearable biosensors under NRF/CRP-8 Program-Self powered body sensor network for disease management and prevention-oriented healthcare.

REFERENCES

- [1] Beeby S P, Torah R N, Tudor M J, Glynne-Jones P, O'Donnell T, Saha C R and Roy S 2007 A micro electromagnetic generator for vibration energy harvesting *J. Micromech. Microeng.* **17** 1257–65
- [2] Elfrink R, Kamel T M, Goedbloed M, Matova S, Hohlfeld D, van An del Y and van Schaijk R 2009 Vibration energy harvesting with aluminum nitride-based piezoelectric devices *J. Micromech. Microeng.* **19** 094005
- [3] Basset P, Galayko D, Paracha A M, Marty F, Dudka A and Bourouina T 2009 A batch-fabricated and electret-free silicon electrostatic vibration energy harvester *J. Micromech. Microeng.* **19** 115025
- [4] Hoffmann D, Folkmer B and Manoli Y 2009 Fabrication, characterization and modelling of electrostatic micro-generators *J. Micromech. Microeng.* **10** 094001
- [5] Zhu D, Tudor M J and Beeby S P 2010 Strategies for increasing the operating frequency range of vibration energy harvesters: a review *Meas. Sci. Technol.* **21** 022001
- [6] Tang L, Yang Y and Soh C K 2010 Towards Broadband Vibration-based Energy Harvesting *J. Intell. Mater. Syst.* **21** 1867-97
- [7] Xing X, Lou J, Yang G M, Obi O, Driscoll C and Suna N X 2009 Wideband vibration energy harvester with high permeability magnetic material *Appl. Phys. Lett.* **99** 083105
- [8] Liu H, Tay C J, Quan C, Kobayashi T and Lee C 2011 Piezoelectric MEMS energy harvester for low-frequency vibrations with wideband operation range and steadily increased output power *J. Microelectromech. Syst.* **20** 1225–7
- [9] Nguyen S D and Halvorsen E 2011 Nonlinear springs for bandwidth-tolerant vibration energy harvesting *J. Microelectromech. Syst.* **20** 1225–7
- [10] Reilly E, Miller L, Fain R, and Wright P K 2009 A study of ambient vibrations for piezoelectric energy conversion *Proceedings of PowerMEMS 2009* 312-5
- [11] Bartsch U, Gaspar J and Paul O 2010 Low-frequency two-dimensional resonators for vibrational micro energy harvesting *J. Micromech. Microeng.* **20** 035016